JCI insight

Amendment history:
- Corrigendum (April 2019)

Thymosin α-1 does not correct F508del-CFTR in cystic fibrosis airway epithelia

Valeria Tomati, Emanuela Caci, Loretta Ferrera, Emanuela Pesce, Elvira Sondo, Deborah M. Cholon, Nancy L. Quinney, Susan E. Boyles, Andrea Armirotti, Roberto Ravazzolo, Luis J.V. Galietta, Martina Gentzsch, Nicoletta Pedemonte

JCI Insight. 2018;3(3):e98699. https://doi.org/10.1172/jci.insight.98699.

Research Article **Therapeutics**

In cystic fibrosis (CF), deletion of phenylalanine 508 (F508del) in the cystic fibrosis transmembrane conductance regulator (CFTR) anion channel causes misfolding and premature degradation. Considering the numerous effects of the F508del mutation on the assembly and processing of CFTR protein, combination therapy with several pharmacological correctors is likely to be required to treat CF patients. Recently, it has been reported that thymosin α-1 (Tα-1) has multiple beneficial effects that could lead to a single-molecule-based therapy for CF patients with F508del. Such effects include suppression of inflammation, improvement in F508del-CFTR maturation and gating, and stimulation of chloride secretion through the calcium-activated chloride channel (CaCC). Given the importance of such a drug, we aimed to characterize the underlying molecular mechanisms of action of Tα-1. In-depth analysis of Tα-1 effects was performed using well-established microfluorimetric, biochemical, and electrophysiological techniques on epithelial cell lines and primary bronchial epithelial cells from CF patients. The studies, which were conducted in 2 independent laboratories with identical outcome, demonstrated that Tα-1 is devoid of activity on mutant CFTR as well as on CaCC. Although Tα-1 may still be useful as an antiinflammatory agent, its ability to target defective […]

JCI insight

RESEARCH ARTICLE

Thymosin α-1 does not correct F508del-CFTR in cystic fibrosis airway epithelia

Valeria Tomati,[1] Emanuela Caci,[1] Loretta Ferrera,[1] Emanuela Pesce,[1] Elvira Sondo,[1] Deborah M. Cholon,[2] Nancy L. Quinney,[2] Susan E. Boyles,[2] Andrea Armirotti,[3] Roberto Ravazzolo,[1,4] Luis J.V. Galietta,[5] Martina Gentzsch,[2,6] and Nicoletta Pedemonte[1]

[1]U.O.C. Genetica Medica, Istituto Giannina Gaslini, Genova, Italy. [2]Marsico Lung Institute/Cystic Fibrosis Research Center, University of North Carolina at Chapel Hill, Chapel Hill, North Carolina, USA. [3]Fondazione Istituto Italiano di Tecnologia, Analytical Chemistry Lab, Genova, Italy. [4]University of Genova, DINOGMI Department, Genova, Italy. [5]Telethon Institute for Genetics and Medicine (TIGEM), Pozzuoli, Italy. [6]Department of Cell Biology and Physiology, University of North Carolina at Chapel Hill, Chapel Hill, North Carolina, USA.

In cystic fibrosis (CF), deletion of phenylalanine 508 (F508del) in the cystic fibrosis transmembrane conductance regulator (CFTR) anion channel causes misfolding and premature degradation. Considering the numerous effects of the F508del mutation on the assembly and processing of CFTR protein, combination therapy with several pharmacological correctors is likely to be required to treat CF patients. Recently, it has been reported that thymosin α-1 (Tα-1) has multiple beneficial effects that could lead to a single-molecule-based therapy for CF patients with F508del. Such effects include suppression of inflammation, improvement in F508del-CFTR maturation and gating, and stimulation of chloride secretion through the calcium-activated chloride channel (CaCC). Given the importance of such a drug, we aimed to characterize the underlying molecular mechanisms of action of Tα-1. In-depth analysis of Tα-1 effects was performed using well-established microfluorimetric, biochemical, and electrophysiological techniques on epithelial cell lines and primary bronchial epithelial cells from CF patients. The studies, which were conducted in 2 independent laboratories with identical outcome, demonstrated that Tα-1 is devoid of activity on mutant CFTR as well as on CaCC. Although Tα-1 may still be useful as an antiinflammatory agent, its ability to target defective anion transport in CF remains to be further investigated.

Introduction

Cystic fibrosis (CF), the most frequent genetic disease in the Caucasian population (1 child affected in nearly 3,000 births), causes meconium ileus, deterioration of lung function, pancreatic insufficiency, and male infertility (1). CF is caused by loss-of-function mutations in the gene encoding the cystic fibrosis transmembrane conductance regulator (CFTR) (2), an ATP-binding cassette (ABC) transporter expressed at the apical membrane of many epithelia, which functions as an ATP-gated anion channel (3). Approximately 2,000 mutations, most of them being very rare, have been identified in the *CFTR* gene (http://www.genet.sickkids.on.ca/app), but only a subset of them lead to a defective protein or manifest as a clinical phenotype (4).

The most common CF mutation (~60% of all CF alleles worldwide with relevant ethnic variability) is the deletion of phenylalanine 508 (F508del). This mutation reduces the intrinsic stability of the first nucleotide-binding domain (NBD1) and perturbs interactions between NBD1 and NBD2 as well as those between NBD1 and the membrane-spanning domains (MSDs) (5). Such abnormalities lead to misfolding of F508del-CFTR, ubiquitination in the endoplasmic reticulum (ER), and premature degradation by the proteasome (6, 7). A small fraction of F508del-CFTR molecules reaches the plasma membrane but exhibits reduced stability (8) and defective channel gating (9).

To address the basic defects of F508del-CFTR, 2 different types of molecules are required, namely CFTR correctors to increase the amount F508del-CFTR protein at the plasma membrane, and CFTR potentiators to improve channel gating (i.e., function) (5, 10). A combination drug containing 1 corrector and 1 potentiator can restore transepithelial chloride transport to CF airway epithelia expressing F508del-CFTR, improving hydration and restoring mucociliary clearance (11). At present, 2 drugs targeting mutant CFTR are available for CF patients: the CFTR corrector lumacaftor (VX-809) and the CFTR potentiator

Authorship note: VT, EC, and LF contributed equally to this work.

Conflict of interest: The authors have declared that no conflict of interest exists.

Submitted: November 15, 2017
Accepted: December 28, 2017
Published: February 8, 2018

Reference information:
JCI Insight. 2018;3(3):e98699. https://doi.org/10.1172/jci.insight.98699.

ivacaftor (VX-770) (11, 12). While the mechanism of action of VX-809 is still under investigation, it has been demonstrated that VX-770 potentiates CFTR function in a phosphorylation-dependent but ATP-independent manner (13) by promoting decoupling between the gating cycle and ATP hydrolysis cycle (14). Ivacaftor is approved for use with 33 CF mutations that disrupt gating and/or reduce function (https://www.fda.gov/NewsEvents/Newsroom/PressAnnouncements/ucm559212.htm). For the more predominant population of CF patients homozygous for F508del-CFTR, the less effective lumacaftor-ivacaftor combination therapy (Orkambi) is available (15).

CFTR potentiators are believed to directly bind to mutant CFTR, favoring channel opening (10). By contrast, some CFTR correctors act as pharmacological chaperones while others are proteostasis regulators (16–18). Pharmacological chaperones act by stabilizing specific CFTR domains and/or improving the interactions of different CFTR domains (19). Proteostasis regulators modulate the proteostasis environment, leading to beneficial effects on CFTR processing and plasma membrane stability (17). Regardless of their mechanism of action, the use of a single CFTR corrector is insufficient to achieve therapeutically relevant rescue of F508del-CFTR (19, 20). Early studies of CFTR correctors identified a threshold in the maximal correction achieved with a single drug of about 20% wild-type (WT) CFTR function (21, 22). An explanation for the limited effectiveness of first-generation CFTR correctors is the presence of multiple defects caused by the F508del mutation, a situation that requires combinations of correctors having complementary mechanisms of action to achieve very effective mutant CFTR rescue (23, 24).

Very recently, it has been reported that thymosin α-1 (Tα-1), a naturally occurring polypeptide acting as an immunomodulator (25), represents a potential single-molecule-based therapy for cystic fibrosis (26). Indeed, Romani and colleagues showed that Tα-1 reduces inflammation and increases CFTR maturation, stability, and activity, thus completely reverting pathological phenotypes due to F508del-CFTR mutants, both in vitro, in the CFBE41o- cell line and in human primary bronchial epithelia, and in vivo, in a CF mouse model (26). Such a drug would be of primary importance for CF patients. Tα-1 also appeared to promote the function of the compensatory calcium-activated chloride channel (CaCC). This type of activity could make Tα-1 also suitable for the therapy of all CF patients, irrespective of their CFTR genotype. To characterize the mechanism of action of Tα-1, we have undertaken an in-depth analysis of its activity using well-established biochemical and functional methods, conducted in 2 independent laboratories. Contrary to expectations, our results indicate that Tα-1 is devoid of activity on mutant CFTR and CaCC.

Results

Tα-1 does not increase F508del-CFTR expression/function in primary bronchial epithelia derived from CF patients as evidenced by electrophysiological and biochemical techniques. It has been reported that 24-hour treatment with Tα-1 causes an increase in the expression of mature (fully glycosylated) CFTR, paralleled by an increase in CFTR function and potentiation of CaCC activity (as evidenced by microfluorimetric and electrophysiological assays including short-circuit current measurements and patch-clamp analysis) (26). We tested Tα-1 on well-differentiated primary cultures of human bronchial epithelial cells from 3 different F508del homozygous subjects by using electrophysiological and biochemical techniques (Figure 1). To this end, bronchial cells were seeded on permeable supports and cultured until cells polarized and differentiated under air-liquid interface conditions. Bronchial epithelia were then treated for 24 hours (Figure 1, A–F) and 48 hours (Figure 1, G and I) with DMSO vehicle alone, with Tα-1 (100 ng/ml) or scrambled peptide (100 ng/ml), or with VX-809 (3 μM). In parallel, we also treated bronchial epithelia with cysteamine (250 μM), whose corrector activity occurs through the same pathway involved in the rescue of F508del-CFTR by Tα-1 (27, 28). After treatment, epithelia were mounted in Ussing chambers for measurement of chloride secretion by short-circuit current analysis (Figure 1, A–E). After blocking Na^+ current with amiloride, cells treated with DMSO vehicle alone or scrambled peptide showed little CFTR function, as indicated by the response to the membrane-permeant cAMP analog CPT-cAMP and the potentiator VX-770. The low activity of F508del-CFTR in the apical membrane was confirmed by the relatively small current drop caused by the selective CFTR inhibitor, $CFTR_{inh}$-172 (29). Conversely, stimulation with UTP elicited a marked transient response that corresponds to activation of CaCCs. As expected, incubation with VX-809 (3 μM), a well-known corrector of F508del-CFTR (11) at 37°C for 24 hours resulted in significant F508del-CFTR rescue. This is evident from the large current increase elicited by the addition of CPT-cAMP and VX-770 and the amplitude of the block caused by $CFTR_{inh}$-172. As also expected, no differences were observed in the amplitude of the UTP-stimulated current, which reflects the activation of CaCCs. Intriguingly, epithelia treated with Tα-1 showed no significant change

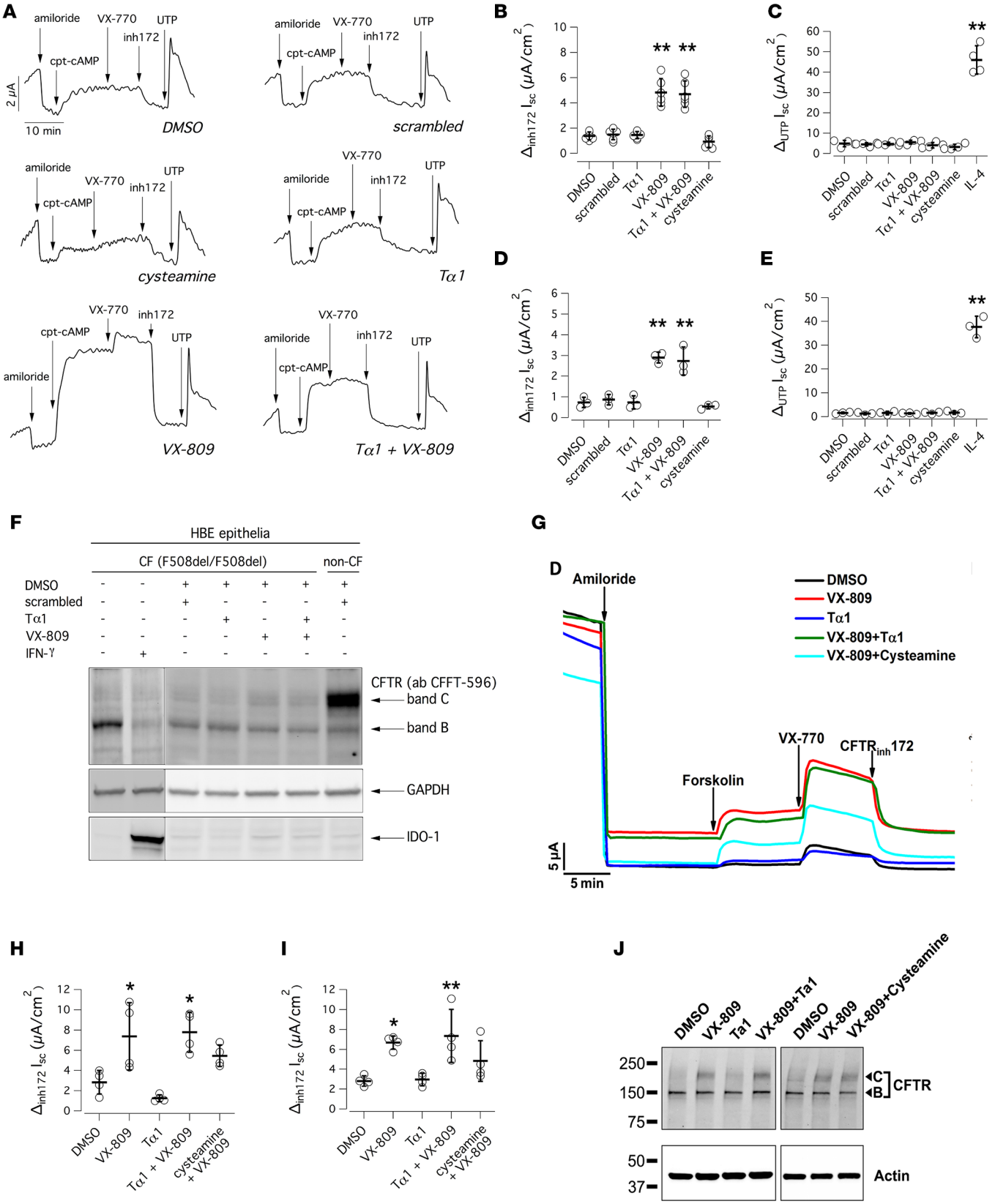

Figure 1. Evaluation of thymosin α-1 (Tα-1) effect on F508del-CFTR activity and expression pattern on human primary bronchial epithelia (HBE) derived from CF patients. (**A**) Representative traces from Ussing chamber recordings of HBE derived from a homozygous F508del patient (donor code BE93) following a 24-hour treatment with DMSO alone (0.1%), scrambled peptide (100 ng/ml + 0.1% DMSO), Tα-1 (100 ng/ml + 0.1% DMSO), VX-809 (3 μM), Tα-1 plus VX-809, or cysteamine (250 μM). (**B**–**E**) Dot plots summarizing CFTR-mediated (**B** and **D**) and CaCC-mediated (**C** and **E**) currents from Ussing chamber recordings of HBE derived from 2 homozygous F508del patients (**B** and **C**, donor code BE91; **D** and **E**, donor code BE115) treated as described in **A**.

Mean values ± SD are shown (n = 3–6). **P < 0.01 versus negative control by ANOVA. (**F**) Biochemical analysis of the F508del-CFTR expression pattern. The figure shows the electrophoretic mobility of F508del-CFTR in HBE from a F508del homozygous patient (BE93), treated for 24 hours with indicated compounds (concentrations as in **A**) or with IFN-γ (100 U/ml). Arrows indicate complex-glycosylated (band C) and core-glycosylated (band B) forms of CFTR protein. The lower panel shows indoleamine 2,3-dioxygenase 1 (IDO-1) expression in the same samples. Similar results were obtained from epithelia derived from 3 different homozygous F508del patients. (**G**) Representative traces from Ussing chamber recordings of HBE derived from 2 different homozygous F508del patients performed in a second independent laboratory. Epithelia cultures were treated with vehicle (DMSO), cysteamine (250 μM), Tα-1 (100 ng/ml), VX-809 (5 μM), cysteamine plus VX-809, or Tα-1 plus VX-809 for 48 hours. (**H** and **I**) Dot plots summarizing CFTR-mediated currents from Ussing chamber recordings of HBE derived from 2 homozygous F508del patients (**H**, donor code KK012B; **I**, donor code KKCFFT004K) treated as described in **G**. Analysis of variance was calculated for the groups. Mean values ± SD are shown (n = 4). *P < 0.05 versus negative control by ANOVA. (**J**) Biochemical analysis of the F508del-CFTR expression pattern in HBE from a F508del homozygous patient, treated for 48 hours as indicated in **G**. To enhance detection of band C, CFTR was immunoprecipitated from lysates with rabbit anti-CFTR antibody 155 and then detected by Western blot analysis utilizing antibody CFFT-596. Arrows indicate complex-glycosylated (band C) and core-glycosylated (band B) forms of CFTR protein.

in CFTR-dependent and CaCC-dependent function as compared with DMSO- or scrambled peptide–treated epithelia (Figure 1, A–E). For comparison, epithelia treated for 24 hours with 10 ng/ml IL-4, a strong inducer of TMEM16A, the protein responsible for CaCC function (30), displayed a 10-fold increase in the UTP-dependent current (Figure 1, C and E).

We also investigated mutant CFTR maturation in the same F508del/F508del bronchial epithelia. To this end, epithelia were treated for 24 or 48 hours with test compounds, lysed and analyzed, after separation by SDS-PAGE, by Western blotting (Figure 1F). In Western blots, CFTR protein is detected as 2 bands, named B and C, of approximately 150 and 170 kDa, respectively. Band B corresponds to partially glycosylated CFTR residing in the ER. Band C is instead the mature fully processed CFTR that has passed through the Golgi. The prevalent form in cells expressing WT CFTR is band C. Lysates of cells expressing F508del-CFTR show primarily band B, consistent with the severe trafficking defect caused by the mutation. In agreement with functional data, we observed an increase in the expression of the mature form of CFTR following treatment of epithelia with VX-809 as compared with control conditions (epithelia treated with DMSO or scrambled peptide; see Figure 1F). However, no detectable change in the appearance of band C was observed following treatment of epithelia with Tα-1. Intriguingly, treatment of primary bronchial epithelia with Tα-1 did not elicit indoleamine 2,3-dioxygenase 1 (IDO-1) expression (Figure 1F). However, a marked increase of this enzyme could be detected following a 24-hour incubation with IFN-γ (100 U/ml), as described in the literature by our and other research groups (31, 32). Concomitantly, incubation with IFN-γ downregulated CFTR expression (Figure 1F), as previously reported (33, 34). Similar functional and biochemical results were obtained independently by a second laboratory (Martina Gentzsch and colleagues, University of North Carolina at Chapel Hill) performing short-circuit current measurements (Figure 1, G–I) and Western blot analysis (Figure 1J) on human bronchial epithelia derived from 2 different F508del homozygous CF patients.

Tα-1 does not increase F508del-CFTR function as determined by the YFP-based microfluorimetric assay in immortalized bronchial CFBE41o- cells. We then tested the ability of Tα-1 to rescue mutant CFTR on immortalized bronchial cells, the CFBE41o- bronchial epithelial cell line, stably expressing F508del-CFTR (35). Indeed, endogenous CFTR expression in parental CFBE41o- cells is negligible. F508del-CFTR CFBE41o- cells were subsequently engineered to stably express the halide-sensitive yellow fluorescent protein (HS-YFP). This cell line has been extensively used by our group to identify and characterize various CFTR modulators, including proteostasis regulators (36–40). CFBE41o- cells, coexpressing F508del-CFTR and HS-YFP, plated on 96-well plates, were treated for 24 hours with vehicle alone (DMSO), Tα-1 (25, 50, 100, or 200 ng/ml, all containing the same amount of DMSO), scrambled peptide (100 ng/ml, also containing DMSO), or cysteamine (250 μM). As a positive control, we treated cells with VX-809 (3 μM). We also tested combined treatment with VX-809 (3 μM) plus Tα-1 at different concentrations. After 24 hours, F508del-CFTR activity in the plasma membrane was assessed by measuring the rate of HS-YFP quenching caused by iodide influx into cells (Figure 2A). Corrector VX-809 caused a marked increase in the rate of fluorescence quenching as compared with control conditions (Figure 2A). In contrast, the YFP quenching rate was unaltered in cells treated with Tα-1 alone or Tα-1 plus VX-809 as compared with cells treated with scrambled peptide or VX-809 alone, respectively (Figure 2A). Similarly, cysteamine was not effective in rescuing F508del-CFTR activity (Figure 2A). We then tested the same compounds on a second cell line widely used to study CFTR modulators, FRT cells stably overexpressing F508del-CFTR (21, 22), obtaining similar results (Figure 2B).

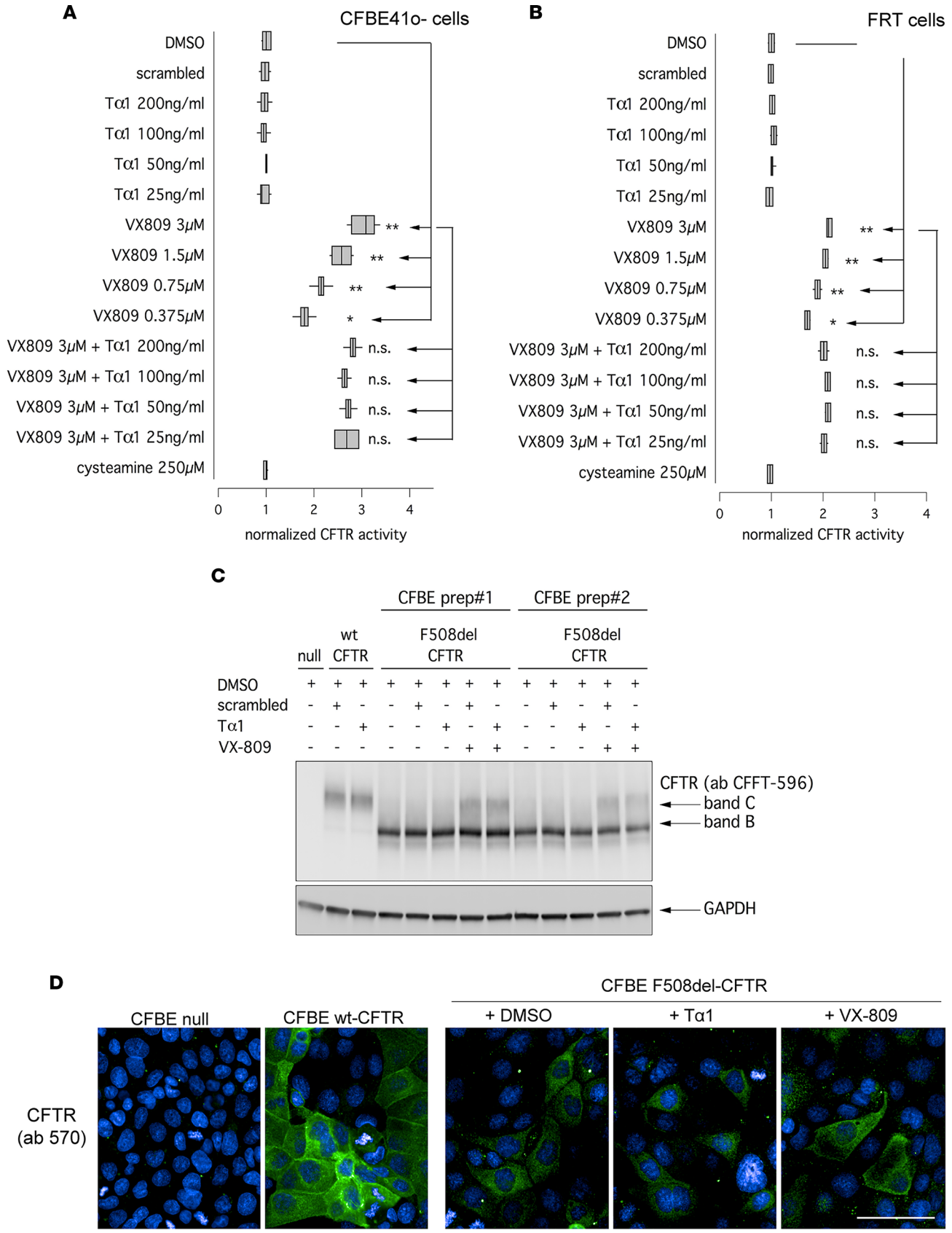

Figure 2. Evaluation of thymosin α-1 (Tα-1) effect on F508del-CFTR activity and expression pattern on immortalized bronchial CFBE41o- cells. (**A** and **B**) Box-and-whisker plot showing F508del-CFTR activity in CFBE41o- cells (**A**) or FRT cells (**B**) based on the YFP assay, showing iodide influx in the presence or absence of F508del-CFTR function rescue in cells treated for 24 hours with DMSO alone (0.1%), scrambled peptide (100 ng/ml + 0.1% DMSO), Tα-1 (100 ng/ml + 0.1% DMSO), VX-809 (3 μM), or Tα-1 plus VX-809. The bounds of the box are the 25th and 75th percentiles, the central line is the median, and the whiskers

are the minimum and maximum values ($n = 9$). *$P < 0.05$, **$P < 0.01$ versus negative control by ANOVA. n.s., not significant. (**C**) Biochemical analysis of the F508del-CFTR expression pattern. The figures show the electrophoretic mobility of F508del-CFTR in 2 different preparations of CFBE41o- cells, treated for 24 hours with the indicated compounds (concentrations as in **A**). Arrows indicate complex-glycosylated (band C) and core-glycosylated (band B) forms of CFTR protein. (**D**) Confocal microscopy images showing immunolocalization of WT-CFTR or F508del-CFTR protein in CFBE41o- cells following 24-hour treatment with DMSO alone (0.1%), Tα-1 (100 ng/ml + 0.1% DMSO), or VX-809 (3 μM), as detected by the anti-CFTR CFFT-570 antibody. Images from parental CFBE41o- cells are also shown for comparison. Scale bar: 100 μm.

Tα-1 does not improve the maturation of F508del-CFTR in immortalized CFBE41o- bronchial epithelial cells. The maturation of F508del-CFTR was also investigated in CFBE41o- cells. As expected, lysates of cells expressing F508del-CFTR showed primarily band B, consistent with the severe trafficking defect caused by the mutation (Figure 2C). No bands were detected in parental CFBE41o- cells, consistent with the loss of endogenous CFTR expression in this cell line. To evaluate the effect of Tα-1 on F508del-CFTR protein, we treated CFBE41o- (expressing F508del-CFTR) with DMSO, with Tα-1 (100 ng/ml) or scrambled peptide (100 ng/ml), or with VX-809 (3 μM). The following day, cells were lysed and lysates were analyzed by SDS-PAGE followed by Western blotting (Figure 2C). For each lane, CFTR bands, analyzed as regions of interest (ROI), were quantified after normalization to GAPDH to account for total protein loading. Treatment of F508del-CFTR cells with corrector VX-809 markedly enhanced expression of mature CFTR (band C). However, no differences were observed following incubation with Tα-1 (Figure 2C).

Tα-1 does not modify F508del-CFTR subcellular localization. We further analyzed the rescue of F508del-CFTR using immunofluorescence in CFBE41o- cells. To immunodetect CFTR we used the Cystic Fibrosis Foundation Therapeutics (CFFT) antibody 570 (41–45). As expected, in parental CFBE41o- cells it was not possible to detect any protein expression. In contrast, in CFBE41o- cells expressing WT CFTR, a marked staining of the cell periphery was observed, in agreement with a predominant localization of the protein in the plasma membrane. In CFBE41o- cells expressing F508del-CFTR, the signal appeared to be largely localized to intracellular compartments (Figure 2D). In F508del-CFTR CFBE41o- cells treated with Tα-1 (100 ng/ml) the localization of the mutant was similar to the one observed in vehicle-treated cells. Only following treatment with VX-809 was the pattern of F508del-CFTR expression modified, consisting of an enhanced localization to the plasma membrane (Figure 2D).

Tα-1 does not alter F508del-CFTR or CaCC currents as evidenced by single-cell electrophysiological techniques. To further investigate the effect of Tα-1 on the expression and function of mutant CFTR and CaCCs, we performed experiments using the whole-cell patch-clamp technique on CFBE41o- cells stably expressing F508del-CFTR. These cells also have endogenous expression of CaCCs, i.e., TMEM16A (30). We incubated the cells for 24 hours with VX-809 (3 μM), Tα-1 (100 ng/ml), or scrambled peptide (100 ng/ml). During patch-clamp recordings, the cells were acutely stimulated with forskolin (20 μM) plus genistein (30 μM) to fully activate F508del-CFTR in the plasma membrane. In cells treated with VX-809, this stimulation led to the appearance of membrane currents with linear current-voltage relationships as expected for CFTR channels (Figure 3, A and B). Furthermore, the reversal potential of such currents was close to –40 mV, in agreement with the activity of a Cl^--selective conductance under our experimental conditions (151 mM Cl^- extracellular, 30 mM Cl^- intracellular). Importantly, such currents were markedly reduced and the reversal potential shifted to zero upon addition of $CFTR_{inh}$-172. In contrast, cells treated with Tα-1 (100 ng/ml) were indistinguishable from those treated with the scrambled peptide. Indeed, there was negligible response to the stimulating cocktail and to $CFTR_{inh}$-172 (Figure 3, A and B). Importantly, the reversal potential in cells treated with Tα-1 was essentially close to zero as in control-treated cells, irrespective of stimulation with forskolin/genistein or inhibition with $CFTR_{inh}$-172. Such results indicate negligible rescue by Tα-1.

To study CaCC function, we acutely stimulated CFBE41o- cells with ionomycin (500 nM), an ionophore that increases intracellular Ca^{2+} concentration. Ionomycin elicited voltage-dependent currents with the typical appearance of CaCCs (Figure 3, C and D). Such currents were of similar amplitude irrespective of treatment (DMSO, Tα-1, or scrambled peptide). Also, niflumic acid (100 μM), a blocker of CaCCs, had a similar effect on all cells (Figure 3, C and D). Such results reveal that Tα-1 is not effective on CaCC function.

Evaluation of Tα-1 sequence and its effect on proliferation and apoptosis of MCF-7 breast cancer cells. Given the unexpected negative results, we performed an LC-MS/MS sequence analysis of the synthetic Tα-1 peptides used for our studies (obtained from 2 different commercial sources). The analysis fully confirmed the

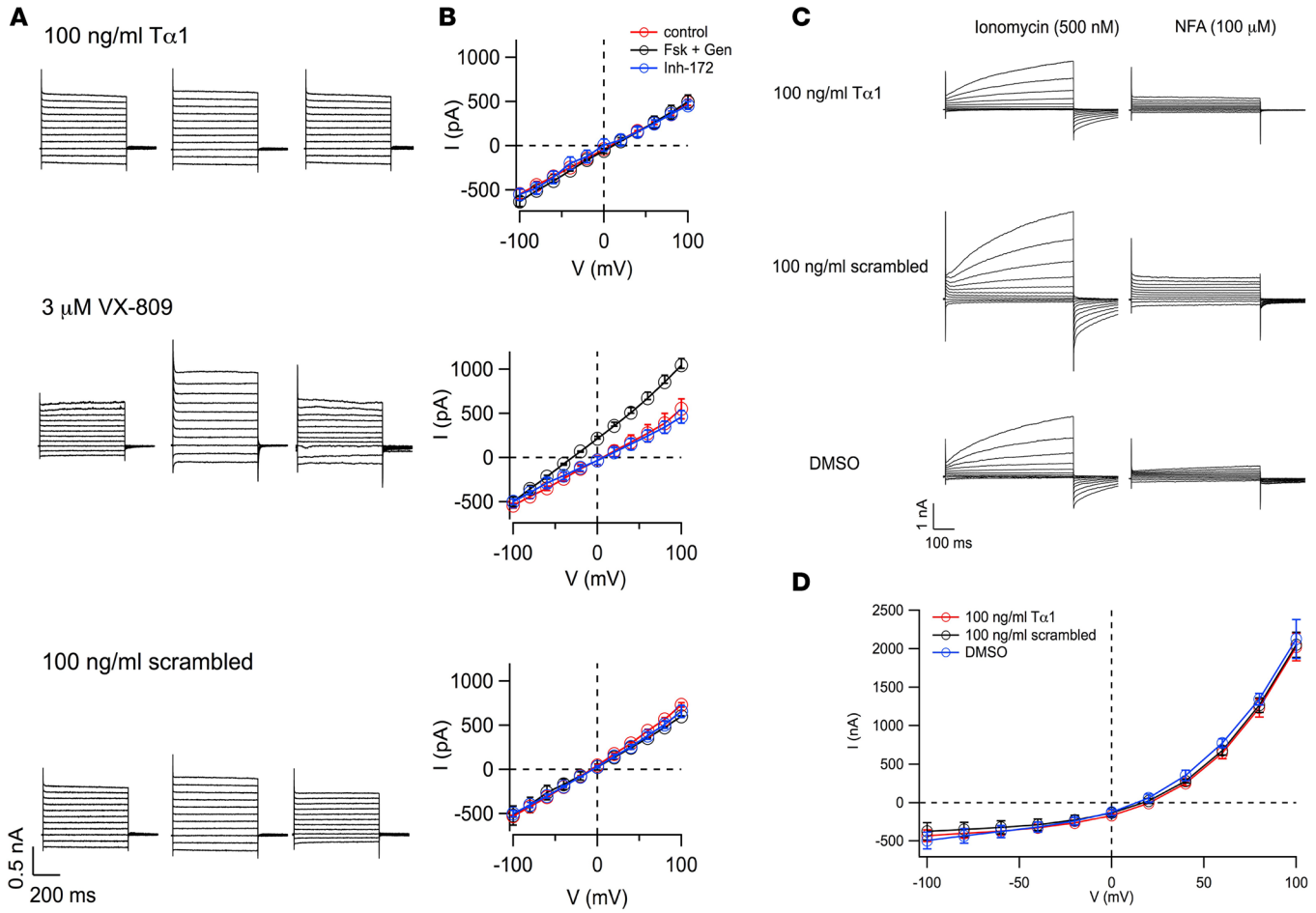

Figure 3. Evaluation of thymosin α-1 (Tα-1) effect on F508del-CFTR and CaCC channel currents performed by whole-cell patch-clamp analysis on immortalized bronchial CFBE41o- cells. (**A**) Representative whole-cell membrane currents and corresponding current–voltage relationships from patch-clamp experiments on F508del-CFTR expressing CFBE41o- cells treated for 24 hours with scrambled peptide (100 ng/ml + 0.1% DMSO), Tα-1 (100 ng/ml + 0.1% DMSO), or VX-809 (3 μM). The recordings were performed first on cells under resting conditions, after maximal CFTR stimulation with forskolin (Fsk, 20 μM) plus genistein (Gen, 30 μM) and after CFTR inhibition by $CFTR_{inh}$-172 (1 μM). Each panel shows superimposed currents elicited at membrane potentials in the range –100 to +100 mV. (**B**) Current–voltage relationships corresponding to data from patch-clamp experiments performed as described in **A**. (**C**) Representative whole-cell membrane currents from patch-clamp experiments on CFBE41o- cells treated for 24 hours with DMSO alone (0.1%), scrambled peptide (100 ng/ml + 0.1% DMSO), or Tα-1 (100 ng/ml + 0.1% DMSO). The recordings were performed after acute treatment with ionomycin (500 nM) to maximally stimulate CaCC activity and after CaCC inhibition by niflumic acid (NFA) (100 μM). Each panel shows superimposed currents elicited at membrane potentials in the range –100 to +100 mV. (**D**) Current–voltage relationships corresponding to data from patch-clamp experiments performed as described in **C**.

sequence of the synthetic Tα-1 peptides (Supplemental File 1). We then evaluated the effect of chronic treatment with Tα-1 on the proliferation and apoptosis of MCF-7 breast cancer cells. Indeed, various research groups reported that long-term treatment (72 hours) with Tα-1 (in the 150–500 μM concentration range) decreases the proliferation rate of MCF-7 and causes cell apoptosis (46, 47). Therefore, we plated MCF-7 at low density on 96-well plates suitable for confocal high-content imaging and evaluated cell proliferation for 72 hours following treatment with Tα-1 (100 ng/ml) or scrambled peptide (100 ng/ml). At the end, we counterstained cell nuclei with Hoechst 33342 and propidium iodide to visualize total cell counts and apoptotic cell counts, respectively. We found that long-term treatment with Tα-1 caused a 50% decrease in cell proliferation, as compared with the control condition (Figure 4A). At the same time, the number of apoptotic cells increased by 22-fold (Figure 4B). These results are in agreement with the findings of other authors (46, 47).

Validation of the CF3 antibody. We wondered whether the lack of CFTR rescue observed in our laboratories using biochemical techniques could be due to the different antibody used as compared with Romani and collaborators (26), using CF3 antibody originally developed by Pier and collaborators (48).

We first tested the CF3 antibody in CFTR immunolocalization studies. The CF3 antibody was used under the same conditions used by Romani and collaborators (26). Surprisingly and unexpectedly, the CF3 antibody

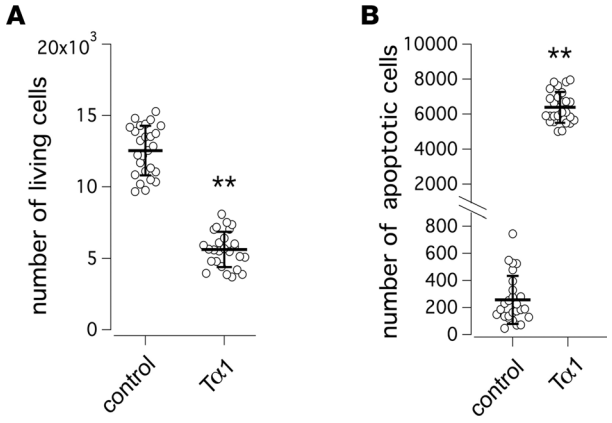

Figure 4. Evaluation of thymosin α-1 (Tα-1) effect on proliferation and apoptosis of MCF-7 breast cancer cells. (**A**) Dot plot showing proliferation of MCF-7 cells after 72-hour treatment with Tα-1 (100 ng/ml) or scrambled peptide (100 ng/ml, control). (**B**) Dot plot showing the number of apoptotic MCF-7 cells after 72-hour treatment with Tα-1 (100 ng/ml) or scrambled peptide (100 ng/ml, control). Mean values ± SD are shown (n = 26). $^{**}P < 0.01$ versus negative control by ANOVA.

revealed a cytosolic signal that was the same in all cells, regardless of the type of CFTR protein (WT vs. mutant) and pharmacological treatment (Figure 5A). In addition, the same signal was also present in parental CFBE41o- cells. Therefore, we first decided to confirm CFTR expression levels in the different CFBE41o- cell lines as assessed by real-time quantitative PCR (RT-qPCR) analysis. According to our analysis, relative CFTR mRNA content (normalized for the transcript abundance of the reference gene β2-microglobulin) in parental, WT-, and F508del-CFTR CFBE41o- cell lines are equal to 6×10^{-5}, 5.2×10^{-2}, and 0.125, respectively. The mRNA expression levels confirmed negligible endogenous expression in parental CFBE41o- cells, not compatible with the signal detected by the CF3 antibody.

Then, we compared the CFTR expression pattern recognized by CF3 antibody with those recognized by highly CFTR-specific CFFT antibodies 570 and 596 (41–45). Parental CFBE41o- cells and CFBE41o- cells with WT-CFTR or F508del-CFTR expression were transfected with nontargeting (NT) or CFTR-specific siRNAs. After 48 hours, cells were lysed and lysates were analyzed by SDS-PAGE followed by Western blotting (Figure 5B). CFFT antibodies 570 and 596 evidenced 2 bands having the classical appearance of CFTR bands: the sharp band at 150 kDa (corresponding to immature, core-glycosylated CFTR, or band B, present in F508del-CFTR cells); and a second, more diffuse, band at 170 kDa, corresponding to mature, fully glycosylated CFTR or band C, present in WT-CFTR cells (Figure 5B). Consistently, the intensity of the 2 bands was markedly reduced in cells in which CFTR was silenced (Figure 5B). In contrast, the CF3 antibody evidenced 1 sharp band at 170 kDa that was present in all lysates, irrespective of CFTR protein version/expression and rescue treatment (Figure 5B).

We also carried out CFTR immunoprecipitation experiments in lysates of parental CFBE41o- cells and CFBE41o- cells with WT-CFTR or F508del-CFTR expression. For this purpose, cells were previously kept under control condition or corrected with VX-809. Immunoprecipitates performed with the anti-CFTR H182 antibody were analyzed by Western blot using the CF3 or the CFFT 596 antibodies in parallel (Figure 5C). Also in this case, the CFFT 596 antibody detected 2 bands resembling the 2 CFTR forms, consistent with the CFTR expression status of the cells analyzed (Figure 5C). Instead, the CF3 antibody detected a single band that was identical in all samples, including the negative control in which the immunoprecipitation step was performed in the absence of the anti-CFTR antibody (Figure 5C). We also performed immunoprecipitation using the CF3 antibody, followed by Western blotting using the CFFT 596 antibody (Figure 5C). The blot demonstrated that the CF3 antibody indeed immunoprecipitated CFTR, which was revealed by the CFFT 596 antibody (Figure 5C).

Finally, we carried out cell surface biotinylation experiments to assess CFTR expression at the plasma membrane detected by CFFT antibody 596 and CF3. Western blot performed on the biotinylated fraction with the CFFT 596 antibody revealed that, in cells expressing WT CFTR, the mature form was prevalent, while cells expressing F508del-CFTR expressed minor levels of immature CFTR on their surface (Figure 5D). This is not surprising, as it has been demonstrated that immature CFTR can traffic to the plasma membrane through the unconventional secretion route (39, 49). Importantly, the levels of mature CFTR available for biotinylation were markedly increased following treatment with VX-809 in F508del-CFTR–expressing cells (Figure 5D). The bands detected in whole lysates by CFFT 596 were consistent with those detected in the biotinylated fraction. In contrast, when Western blot was performed on the biotinylated fraction with the CF3 antibody, a very faint band could be detected at 250 kDa in the lanes corresponding to parental and F508del-CFTR CFBE41o- cells, while

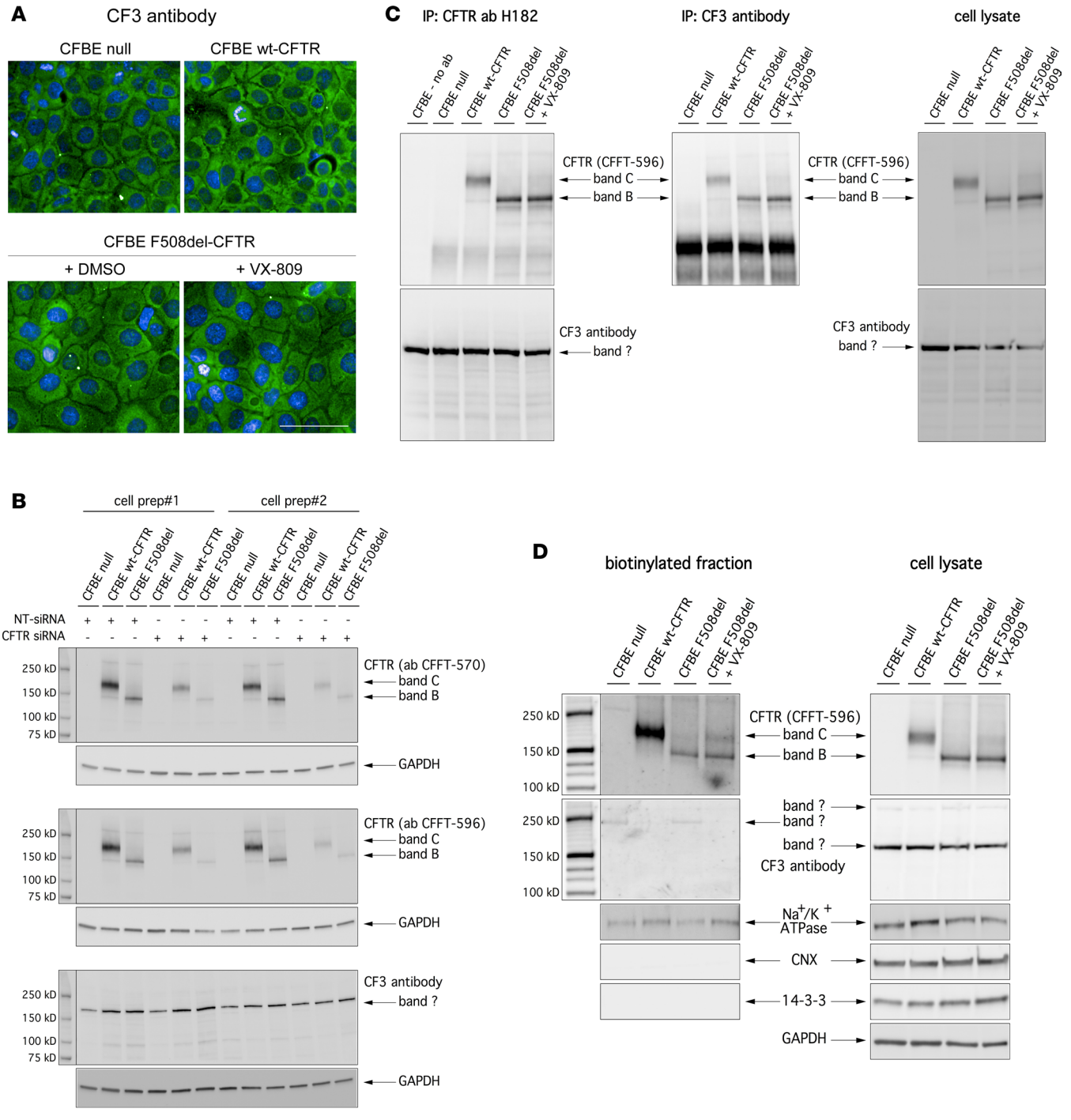

Figure 5. Validation of CF3 antibody. (**A**) Confocal microscopy images showing immunolocalization of WT-CFTR or F508del-CFTR protein in CFBE41o- cells following 24-hour treatment with DMSO alone (0.1%) or VX-809 (3 μM), as detected by the CF3 antibody. Images from parental CFBE41o- cells are also shown for comparison. Scale bar: 100 μm. (**B**) Biochemical analysis of CFTR expression pattern in whole lysates from CFBE41o- cells after transfection with nontargeting (NT) or CFTR-specific siRNA (30 nM final concentration). Immunoblot detection was performed with CFFT-570, CFFT-596, or CF3 antibody as indicated. (**C**) Biochemical analysis of CFTR expression pattern in whole lysates and corresponding immunoprecipitated samples obtained using the anti-CFTR H182 or CF3 antibody. Immunoblot detection of CFTR protein was performed with CFFT-596 or CF3 antibody as indicated. (**D**) Detection by cell surface biotinylation of CFTR forms expressed at the plasma membrane. Immunoblot detection of CFTR (performed with CFFT-596 or CF3 antibody as indicated) and control proteins in the biotinylated fraction and in total lysates from CFBE41o- cells. Absence of the cytosolic proteins calnexin (CNX) and 14-3-3 in the biotinylated fraction confirms surface protein–specific labeling in each experiment.

no bands were detected in the lanes corresponding to WT-CFTR and F508del-CFTR CFBE41o- cells treated with VX-809. In addition, whole lysates of all the samples displayed the same 170-kDa band that was similar in size to mature CFTR, but also present in the parental cells.

Discussion

Pharmacological rescue of processing and trafficking defects caused by the CFTR F508del mutation is a critical goal in CF research. This outcome may be achieved by using pharmacological chaperones that directly interact with mutant CFTR to improve its folding and enhance its stability or by blocking activity of proteins that perturb trafficking and promote its premature degradation. However, the maximal correction achieved by using a single corrector is very limited (21, 22), and combinations of correctors are required to maximize mutant CFTR rescue (23, 24). The finding by Romani and collaborators (26) that the naturally occurring peptide Tα-1 may constitute a single-drug therapy for CF has caught the attention of the CF scientific community and, more importantly, of CF patients. Indeed, this finding has been diffusely reported in the press, creating great expectations (see for example, http://cysticfibrosis.com/thymosin-alpha1/).

Given our interest in the mechanisms involved in CFTR processing and rescue, we were committed to perform in vitro studies aiming to analyze in detail the mechanism of action of Tα-1 as F508del-CFTR corrector, using well-established microfluorimetric, biochemical, and electrophysiological techniques and validated reagents that are widely used by the CF scientific community. We performed functional analysis of Tα-1 activity as F508del-CFTR corrector by means of the microfluorimetric assay based on the HS-YFP that has been extensively used to investigate various rescue maneuvers (36–40) and by means of whole-cell patch-clamp analyses. In parallel, we also performed immunolocalization experiments and biochemical analyses of the electrophoretic mobility of the different CFTR forms expressed by the cells under resting conditions or following treatment with Tα-1. The results obtained with the different techniques unequivocally demonstrated that, in our hands, Tα-1 has no effect on F508del-CFTR maturation, trafficking to the plasma membrane, and function in immortalized bronchial CFBE41o- cells. We also evaluated the effect of Tα-1 on F508del-CFTR processing and function on well-differentiated primary cultures of human bronchial epithelial cells from F508del homozygous patients by using electrophysiological and biochemical techniques. The analyses were performed in 2 independent laboratories, and demonstrated the lack of a Tα-1 effect both on mutant CFTR maturation, and on CFTR-mediated transepithelial chloride secretion. It is interesting to note that we tested cysteamine, a small molecule that has been proposed to rescue F508del-CFTR with a mechanism in common with Tα-1 (26). Cysteamine was also ineffective in our experiments.

As described by Romani and collaborators, the pleiotropic effect of Tα-1 on epithelial anion transport should also involve an increase in the expression/function of CaCCs (26). This is a very important effect because it could also be useful to treat patients with other mutations instead of F508del. Indeed, stimulation of a compensatory anion channel could circumvent the CF basic defect, irrespective of the mutations carried by the patient in the *CFTR* gene. However, we did not observe changes in CaCC activity, as evaluated by electrophysiological techniques in immortalized bronchial CFBE41o- and well-differentiated CF primary bronchial epithelia.

It should be noted that failure to reproduce the results obtained by Romani and collaborators, at least at the biochemical level, can be due to the use of specific reagents. Indeed, an in-depth analysis of the CF3 antibody, used by Romani and collaborators, revealed that this antibody is not suitable for immunofluorescence or Western blot analysis of whole-cell lysates or enriched CFTR samples (i.e., immunoprecipitates or cell surface biotinylated fractions). Indeed, CF3 also appeared to detect other targets unrelated to CFTR expression. Our studies revealed that CF3 can be used for immunoprecipitation, provided that CFTR is then detected by Western blot using well-established antibodies such as those provided by John R. Riordan (University of North Carolina at Chapel Hill) in collaboration with the CFFT (41–45). The importance of verifying the reagents has also recently been highlighted by a notice of the NIH for considering funding (see https://grants.nih.gov/grants/guide/notice-files/NOT-OD-17-068.html).

In conclusion, our findings do not confirm the beneficial effects of Tα-1 on mutant CFTR rescue or compensatory anion channels. However, it is important to note that our studies did not evaluate the impact of Tα-1 as an antiinflammatory agent for CF disease. Therefore, the attenuation of pathological phenotypes observed by Romani and collaborators in the CF mouse model may be related to such activity, and not to CFTR rescue.

Methods

Cell culture. CFBE41o- cells stably expressing WT CFTR or F508del-CFTR alone or together with HS-YFP (YFP-H148Q/I152L) were generated as previously described (35). Culture medium for CFBE41o- cells was as follows: MEM supplemented with 10% FCS, 2 mM L-glutamine, 100 U/ml penicillin, and 100 μg/ml streptomycin. For fluorescence assays of CFTR activity, CFBE41o- cells were plated (50,000 cells/well) on clear-bottom 96-well black microplates (Corning Life Sciences).

MCF-7 (human breast adenocarcinoma cell line; ATCC) were cultured in DMEM medium supplemented with 10% FCS, 2 mM L-glutamine, 100 U/ml penicillin, and 100 μg/ml streptomycin.

The methods for isolation, culture, and differentiation of primary bronchial epithelial cells were previously described in detail (ref. 30; for the laboratory at the Istituto Giannina Gaslini). Briefly, epithelial cells were obtained from mainstem human bronchi, derived from CF individuals undergoing lung transplant. For this study, cells were obtained from 3 CF patients (homozygous for F508del mutation). Cells were detached by overnight incubation of bronchi at 4°C in a protease XIV–containing solution. Epithelial cells were then cultured in a serum-free LHC9-based medium supplemented with various hormones and supplements that favor cell number amplification. For cells derived from CF patients, the culture medium contained in the first days a complex mixture of antibiotics (usually colistin, piperacillin, and tazobactam) to eradicate bacteria.

To obtain differentiated epithelia, cells were seeded at high density on porous membranes (12-mm Snapwell inserts, Corning, code 3801). After 24 hours, the serum-free medium was replaced with DMEM/Ham's F12 containing 2% FBS plus hormones and supplements. Differentiation of cells into a tight epithelium was checked by measuring transepithelial electrical resistance and potential difference with an epithelial voltohmmeter (EVOM1, World Precision Instruments). The medium was replaced daily on both sides of the permeable supports up to 3–5 days (liquid-liquid culture), and then maintained at air-liquid interface for an additional 12 days.

Alternatively, bronchial epithelia cells were cultured as previously described (ref. 50; for the laboratory at the University of North Carolina at Chapel Hill) and seeded on Millicell inserts (12-mm Millipore inserts PICM01250) and maintained at air-liquid interface for 18 days in serum-free BEBM/DMEM (1:1)–based media (51) supplemented with BEGM SingleQuot (Lonza).

Short-circuit current recordings. Snapwell inserts carrying differentiated bronchial epithelia were mounted in a vertical diffusion chamber resembling a Ussing chamber with internal fluid circulation. Both apical and basolateral hemichambers were filled with 5 ml of a solution containing (in mM): 126 NaCl, 0.38 KH_2PO_4, 2.13 K_2HPO_4, 1 $MgSO_4$, 1 $CaCl_2$, 24 $NaHCO_3$, and 10 glucose. Both sides were continuously bubbled with a gas mixture containing 5% CO_2/95% air and the temperature of the solution was kept at 37°C. The transepithelial voltage was short-circuited with a voltage-clamp (DVC-1000, World Precision Instruments) connected to the apical and basolateral chambers via Ag/AgCl electrodes and agar bridges (1 M KCl in 1% agar). The offset between voltage electrodes and the fluid resistance were adjusted to compensate parameters before experiments. The short-circuit current (I_{SC}) was recorded with a PowerLab 4/25 (ADInstruments) analog-to-digital converter connected to a Macintosh computer.

For bronchial epithelia grown on Millicells a VCC MC8 multichannel voltage clamp was utilized, and I_{SC} was measured with Acquire & Analyze Software (Physiologic Instruments) and I_{SC} traces were imported to Origin 9.0.0. (OriginLab Corporation).

Whole-cell patch-clamp recordings. Whole-cell membrane currents were recorded in CFBE41o- cells stably expressing F508del-CFTR channels. The extracellular (bath) solution had the following composition: 145 mM NaCl, 4 mM CsCl 1 mM $CaCl_2$, 10 mM glucose, and 10 mM TES (pH 7.4). For CFTR currents the pipette (intracellular) solution contained 113 mM L-aspartic acid, 113 mM CsOH, 27 mM CsCl, 1 mM NaCl, 1 mM $MgCl_2$, 1 mM EGTA, and 10 mM TES (pH 7.2) plus 3 mM ATP. For CaCC currents pipettes were filled with 130 mM CsCl, 10 mM EGTA, 1 mM $MgCl_2$, 8 mM $CaCl_2$, and 10 mM HEPES.

After a 24-hour incubation with Tα-1 peptide, scrambled peptide, or corrector VX-809 (all containing the same amount of DMSO), stimulation of CFTR-mediated currents was evoked by perfusion with 20 μM forskolin, an adenylyl cyclase activator, plus the potentiator genistein (30 μM). Afterwards, $CFTR_{inh}$-172 (1 μM) was applied by extracellular perfusion, while CaCC currents were stimulated using 500 nM ionomycin and blocked with 100 μM niflumic acid.

During experiments, the membrane capacitance and series resistance were analogically compensated using the circuitry provided by the EPC7 patch-clamp amplifier. The usual protocol for stimulation consisted of

600-ms-long voltage steps from –100 to 100 mV in 20-mV increments starting from a holding potential of –60 mV. The waiting time between steps was 4 seconds. Membrane currents were filtered at 1 kHz and digitized at 5 kHz with an ITC-16 (InstruTECH) AD/DA converter. Data were analyzed using Igor software (Wavemetrics) supplemented by custom software provided by Oscar Moran (Istituto di Biofisica - CNR, Genova, Italy).

Fluorescence assay for CFTR. At the time of the assay, CFBE41o- cells were washed with PBS containing (in mM) 137 NaCl, 2.7 KCl, 8.1 Na_2HPO_4, 1.5 KH_2PO_4, 1 $CaCl_2$, and 0.5 $MgCl_2$. Cells were then incubated for 25 minutes with 60 μl of PBS plus forskolin (20 μM) and VX-770 (1 μM) to maximally stimulate F508del-CFTR. Cells were then transferred to a microplate reader (FluoStar Galaxy; BMG Labtech) for CFTR activity determination. The plate reader was equipped with high-quality excitation (HQ500/20X: 500 ± 10 nm) and emission (HQ535/30M: 535 ± 15 nm) filters for YFP (Chroma Technology). Each assay consisted of a continuous 14-second fluorescence reading 2 seconds before and 12 seconds after injection of 165 μl of an iodide-containing solution (PBS with Cl^- replaced by I^-; final I^- concentration, 100 mM). Data were normalized to the initial background-subtracted fluorescence. To determine I^- influx rate, the final 11 seconds of the data for each well were fitted with an exponential function to extrapolate initial slope (dF/dt).

Evaluation of CFTR mRNA level. To evaluate CFBE41o- cell CFTR mRNA, we extracted total RNA using both TRIzol reagent (Gibco–BRL) and an RNeasy Mini Kit (Qiagen), both following the manufacturers' instructions. One microgram of spectrophotometer-quantified RNA was retrotranscribed using an iScript RT kit (Bio-Rad). RT-qPCR was carried out using inventoried Assays-on-Demand provided by Applied Biosystems. β2-Microglobulin (Hs00187842_m1) served as the reference gene to normalize transcript abundance. RT-qPCR was performed using an IQ5 Real-Time PCR Detection System (Bio-Rad). Cycling conditions were a 3-minute hot start at 95°C, followed by 40 cycles of denaturation at 95°C for 30 seconds, and annealing and extension at 60°C for 30 seconds. mRNA was quantified using the comparative CT method. Each sample was run in triplicate, and data were analyzed using IQ5 Optical System software (Bio-Rad). Changes in transcript levels were quantified using the comparative CT method (Sequence Detection System Chemistry Guide, Applied Biosystems).

Peptides. Tα-1 and scrambled peptide were supplied as purified, sterile, lyophilized, acetylated polypeptides (CRIBI Biotechnology Center, Peptide Facility, Università di Padova, Italy; named as "Vendor A"). The sequences were as follows: Ac-SDAAVDTSSEITTKDLKEKKEVVEEAEN-OH (Tα-1) and Ac-AKSDVKAETSSEIDTTELDEKVEVKANE-OH (scrambled peptide). For in vitro studies, peptides were dissolved in DMSO. As an additional alternative source, Tα-1 peptide was purchased from Abcam (ab42247; named as "Vendor B").

LC-MS/MS sequence analysis of synthetic Tα-1 peptides. Synthetic Tα-1 powders were dissolved at 2 mg/ml in either DMSO (Vendor A) or 0.1% acetic acid (Vendor B), following the Vendor's indications. The sample was then diluted to 10 mg/ml in 3% acetonitrile in water. Two milliliters of this solution was loaded on a nanoAcquity UPLC system coupled to a 5600+ TripleToF mass spectrometer. The samples were desalted on a 180 μm × 20 mm nanoAcquity trapping column and then moved to a 75 μm × 250 mm Picofrit column. Flow rate was set to 300 nl/min. Eluents were A (water + 0.1% formic acid) and B (acetronitrile + 0.1% formic acid). The samples were eluted from the column with a linear gradient of B from 3% to 30% in 15 minutes. Peptides were analyzed in positive nanospray ion mode. Scan range was set from 400 to 1,500 m/z for MS and from 100 to 1,800 m/z for MS/MS. Charge states 3 and 4 precursors were selected for MS/MS. Collision energy profiles were set according to SCIEX settings. The nanoUPLC system and the trapping column were purchased from Waters Inc. The Picofrit column was purchased from Scientific Instruments Service. The TripleToF mass spectrometer was purchased from SCIEX.

Antibodies. The following antibodies were used: mouse monoclonal anti-CFTR (570 and 596, produced, quality tested, and provided by J.R. Riordan through a program of the CFFT; see ref. 44); mouse monoclonal anti-CFTR (clone CF3, originally developed by Pier and collaborators [ref. 48], Abcam, ab2784); rabbit polyclonal anti-CFTR (clone H182, Santa Cruz Biotechnology) and 155 (targeting the C-terminus of CFTR; provided by J.R. Riordan); mouse monoclonal anti–Na^+/K^+ ATPase α1 (clone C464.6, Millipore); rabbit monoclonal anti-calnexin (Abcam, ab22595); rabbit polyclonal anti–14-3-3 zeta (Abcam, ab51129); mouse monoclonal anti-GAPDH (clone 6C5, Santa Cruz Biotechnology); rabbit polyclonal anti–β-actin (Cell Signaling Technology, 4967); horseradish peroxidase (HRP)–conjugated anti–mouse IgG (Abcam); or HRP-conjugated anti-rabbit IgG (DAKO); as well as Alexa Fluor infrared dye–conjugated goat anti-mouse and anti-rabbit IgG (Thermo Fisher Scientific).

Cell surface biotinylation assay. Parental CFBE41o- cells, CFBE41o- cells expressing WT CFTR, or CFBE41o- cells expressing F508del CFTR were treated as previously described (39). Briefly, cells were seeded on 100-mm dishes. The day after, cells were incubated with vehicle alone (0.1% DMSO) or with VX-809 (3 μM). A cell surface biotinylation assay was performed 24 hours later. Briefly, cells were washed twice with ice-cold PBS and incubated twice with biotin (0.35 mg/ml in PBS) for 25 minutes each time on a shaker at 4°C. After 3 washes in PBS, biotin was quenched with 2 washes in NH_4Cl solution (50 mM in PBS, 15 minutes each) on a shaker at 4°C. Cells were then washed 3 times in PBS without Ca^{2+} and Mg^{2+} and then scraped into lysis buffer (50 mM Hepes pH 7, 150 mM NaCl, 1% glycerol, 1% Triton X-100, 1.5 mM $MgCl_2$, 5 mM EGTA). Cell lysates were collected in an Eppendorf tube and rocked for 30 minutes at 4°C. Nuclei were then pelleted by centrifugation at 10,600 *g* at 4°C for 20 minutes. Supernatant protein concentration was calculated using the BCA assay (Euroclone) following the manufacturer's instructions. Then, an aliquot of supernatants corresponding to 600 μg of protein was precipitated by rotating 6 hours at 4°C with high-capacity streptavidin agarose resin (Thermo Fischer Scientific), following the manufacturer's recommendation. The resin was then washed with the following solutions: once with lysis buffer, twice with buffer 1 (150 mM NaCl, 20 mM Tris-HCl, pH 8, 5 mM EDTA, 1% Triton X-100, 0.2% BSA), once with buffer 3 (150 mM NaCl, 20 mM Tris-HCl, pH 8, 5 mM EDTA, 0.5% Triton X-100), and once with buffer 4 (50 mM Tris-HCl, pH 8). Biotinylated proteins were eluted from the resin with 4× reducing sample buffer and 30 μl of each sample was resolved in a 4%–15% or 4%–20% gradient Criterion TGX gel (Bio-Rad) and analyzed by Western blotting.

Western blot. CFBE41o- cells silenced with indicated siRNAs (30 nM final concentration) or treated with vehicle alone (0.1% DMSO) or scrambled peptide (100 ng/ml, also containing the same amount of DMSO) or with Tα-1 (100 ng/ml, also containing DMSO) or with VX-809 (3 μM), were grown to confluence on 60-mm-diameter dishes and lysed in RIPA buffer containing a complete protease inhibitor (Roche). Cell lysates were subjected to centrifugation at 15,300 *g* at 4°C for 10 minutes. Supernatant protein concentration was calculated using the BCA assay (Euroclone) following the manufacturer's instructions. Equal amounts of protein (10 μg to detect CFTR and GAPDH) were resolved in gradient (4%–15% or 4%–20%, depending on target protein molecular weight) Criterion TGX precast gels, transferred to nitrocellulose membranes with a Trans-Blot Turbo system (Bio-Rad), and analyzed by Western blotting. Proteins were detected using the antibodies described above and subsequently visualized by chemiluminescence using the SuperSignal West Femto Substrate (Thermo Fisher Scientific). Chemiluminescence was monitored using the Molecular Imager ChemiDoc XRS System. Images were analyzed with ImageJ software (NIH). Bands were analyzed as ROI, normalized against the GAPDH loading control. Protein bands labeled with Alexa Fluor infrared dye–conjugated IgG were visualized using an Odyssey Infrared Imaging System (LI-COR). See complete unedited blots in the supplemental material.

Immunofluorescence/confocal microscopy. Parental CFBE41o- cells (not expressing CFTR) or CFBE41o- cells expressing native CFTR or expressing F508del CFTR were seeded (50,000 cells/well) on clear-bottom 96-well black microplates suitable for high-content imaging. Twenty-four hours after plating, the medium was changed and the cells were incubated at 37°C for an additional 24 hours with vehicle alone (0.1% DMSO) or scrambled peptide (100 ng/ml, also containing the same amount of DMSO) or with Tα-1 (100 ng/ml, also containing the same amount of DMSO) or with VX-809 (3 μM) prior to fixation.

Cells were washed with PBS and then different protocols were applied depending on the primary antibody used to probe CFTR protein. Cells to be probed with anti-CFTR CFFT antibody 570 were fixed for 5 minutes with Bouin's Solution (HT10132, Sigma-Aldrich). After extensive washing with PBS, cells were permeabilized with PBS/0.3% Triton X-100 and saturated in 1% BSA in PBS for 2 hours. Cells to be probed with the CF3 antibody were fixed with 2% formaldehyde for 15 minutes at room temperature. Subsequently, cells were permeabilized in PBS containing 5% FBS and 3% BSA plus 0.5% Triton X-100 for 5 minutes, and saturated with PBS containing 5% FBS and 3% BSA for 2 hours. Primary antibodies were incubated overnight at 4°C (CFFT antibody 570, 1:500 in 1% BSA in PBS; CF3, 1:100 in PBS containing 5% FBS and 3% BSA). Following incubation with primary antibody, cells were rinsed 3 times in PBS and incubated with Alexa Fluor 488 goat anti–mouse IgG(H+L) (Life Technologies) secondary antibody diluted 1:250 in PBS containing 1% BSA (when the CFFT antibody 570 was used as primary antibody) or PBS containing 5% FBS, 3% BSA (in the case of CF3 antibody) for 1 hour in the dark at room temperature. After a further 3 washes in PBS, cell nuclei

were counterstained with Hoechst 33342. Confocal imaging was performed using an Opera Phenix (PerkinElmer) high-content screening system. Wells were imaged in confocal mode, using a ×40 water-immersion objective. Hoechst 33342 signal was laser excited at 405 nm and the emission was measured between 435 and 550 nm. The Alexa Fluor 488 signal was laser excited at 480 nm and the emission was measured between 500 and 550 nm.

Proliferation study. MCF-7 cells were plated at low density (10,000 cells/well) on 96-well plates suitable for high-content imaging. After 6 hours, cells were treated with the scrambled peptide (100 ng/ml) or with Tα-1 (100 ng/ml). Cell proliferation was monitored for 72 hours using the digital phase contrast channel of the Opera Phenix (PerkinElmer) high-content screening system. At the end of the experiments, cells were counterstained with Hoechst 33342 and propidium iodide to visualize total cells and apoptotic cells, respectively.

Statistics. Due to the fact that more than 2 groups were to be compared, the analysis of variance (ANOVA), followed by a post-hoc test was used in order to avoid multiple-comparisons error. In the case of normally distributed quantitative variables, a parametric ANOVA was performed, whereas when the quantitative variables were skewed, the nonparametric ANOVA (Kruskal-Wallis test) was applied. The Kolmogorov-Smirnov test was used to evaluate the assumption of normality.

Statistical significance of the effect of single treatments on CFTR activity or expression in CFBE41o- cells was tested by parametric 1-way ANOVA followed by the Dunnet multiple comparisons test (all groups against the control group) as post-hoc test. In the case of combination of treatments, statistical significance was verified by ANOVA followed by the Tukey test (for multiple comparisons) as post-hoc test.

Normally distributed data are expressed as the mean ± SD or mean ± SEM as indicated, and significances are 2-sided. Differences were considered statistically significant when P was less than 0.05.

Study approval. The collection of bronchial epithelial cells and their study to investigate the mechanisms of transepithelial ion transport were specifically approved by the Ethics Committee of the Istituto Giannina Gaslini following the guidelines of the Italian Ministry of Health. Each patient provided informed consent to the study using a form that was also approved by the Ethics Committee.

Alternatively, CF human bronchial epithelial cells were isolated from explant lungs under an IRB-approved protocol (03-1396) by the University of North Carolina at Chapel Hill Cystic Fibrosis Center Tissue Procurement and Cell Culture Core. Written informed consent was obtained from all subjects.

Author contributions

Validation of CF3 antibody was performed by VT. Biochemical evaluation of Tα-1 was performed by VT and DMC. Primary bronchial epithelial cells were cultured by EC and SEB. Short-circuit current measurements were performed by EC and NLQ. Patch-clamp analysis was performed by LF. The YFP assay was performed by EP and ES. Analysis of peptide sequence and purity was performed by AA. Functional and biochemical data were analyzed by VT and NP. The study was planned by RR, LJVG, MG, and NP. The manuscript was written by NP with help from RR, MG, and LJVG.

Acknowledgments

We thank John R. Riordan (University of North Carolina at Chapel Hill), and CFFT for kindly providing us with anti-CFTR antibodies. For studies performed in the United States, we thank Scott Randell and the Marsico Lung Institute Tissue Procurement and Cell Culture Core at the University of North Carolina for provision of CF human bronchial epithelial cells. This work was supported by Ricerca Corrente from the Italian Ministry of Health (Linea1); by grants to N. Pedemonte from the Fondazione per la Ricerca sulla Fibrosi Cistica (FFC no. 5/2012 with the contribution of "Danone S.p.A.", and FFC no. 2/2015 with the contribution of "Delegazioni FFC di Verona e di Tradate Gallarate", "La Notte dei Sapori", and "Audemars Piguet Italia"); by the "Task Force for Cystic Fibrosis" strategic project from the Fondazione per la Ricerca sulla Fibrosi Cistica and by Telethon Grant TMLGCBX16TT to L.J.V. Galietta; and by grants supporting the CFF CFTR Functional Analysis Core (BOUCHE15R0) and the NIH Cystic Fibrosis Pre-Clinical Core (NIH P30 DK065988) at the University of North Carolina.

Address correspondence to: Nicoletta Pedemonte, U.O.C. Genetica Medica, Istituto Giannina Gaslini, Via Gerolamo Gaslini 5, 16147 Genova, Italy. Phone: 39.010.56363178; Email: nicoletta.pedemonte@unige.it.

1. Pilewski JM, Frizzell RA. Role of CFTR in airway disease. *Physiol Rev*. 1999;79(1 Suppl):S215–S255.
2. Riordan JR, et al. Identification of the cystic fibrosis gene: cloning and characterization of complementary DNA. *Science*. 1989;245(4922):1066–1073.
3. Hwang TC, Sheppard DN. Gating of the CFTR Cl^- channel by ATP-driven nucleotide-binding domain dimerisation. *J Physiol (Lond)*. 2009;587(Pt 10):2151–2161.
4. Cutting GR. Cystic fibrosis genetics: from molecular understanding to clinical application. *Nat Rev Genet*. 2015;16(1):45–56.
5. Lukacs GL, Verkman AS. CFTR: folding, misfolding and correcting the ΔF508 conformational defect. *Trends Mol Med*. 2012;18(2):81–91.
6. Cheng SH, et al. Defective intracellular transport and processing of CFTR is the molecular basis of most cystic fibrosis. *Cell*. 1990;63(4):827–834.
7. Ward CL, Omura S, Kopito RR. Degradation of CFTR by the ubiquitin-proteasome pathway. *Cell*. 1995;83(1):121–127.
8. Lukacs GL, et al. The delta F508 mutation decreases the stability of cystic fibrosis transmembrane conductance regulator in the plasma membrane. Determination of functional half-lives on transfected cells. *J Biol Chem*. 1993;268(29):21592–21598.
9. Dalemans W, et al. Altered chloride ion channel kinetics associated with the delta F508 cystic fibrosis mutation. *Nature*. 1991;354(6354):526–528.
10. Cai ZW, Liu J, Li HY, Sheppard DN. Targeting F508del-CFTR to develop rational new therapies for cystic fibrosis. *Acta Pharmacol Sin*. 2011;32(6):693–701.
11. Van Goor F, et al. Correction of the F508del-CFTR protein processing defect in vitro by the investigational drug VX-809. *Proc Natl Acad Sci USA*. 2011;108(46):18843–18848.
12. Van Goor F, et al. Rescue of CF airway epithelial cell function in vitro by a CFTR potentiator, VX-770. *Proc Natl Acad Sci USA*. 2009;106(44):18825–18830.
13. Eckford PD, Li C, Ramjeesingh M, Bear CE. Cystic fibrosis transmembrane conductance regulator (CFTR) potentiator VX-770 (ivacaftor) opens the defective channel gate of mutant CFTR in a phosphorylation-dependent but ATP-independent manner. *J Biol Chem*. 2012;287(44):36639–36649.
14. Jih KY, Hwang TC. Vx-770 potentiates CFTR function by promoting decoupling between the gating cycle and ATP hydrolysis cycle. *Proc Natl Acad Sci USA*. 2013;110(11):4404–4409.
15. Wainwright CE, et al. Lumacaftor-ivacaftor in patients with cystic fibrosis homozygous for Phe508del CFTR. *N Engl J Med*. 2015;373(3):220–231.
16. Amaral MD, Farinha CM. Rescuing mutant CFTR: a multi-task approach to a better outcome in treating cystic fibrosis. *Curr Pharm Des*. 2013;19(19):3497–3508.
17. Balch WE, Morimoto RI, Dillin A, Kelly JW. Adapting proteostasis for disease intervention. *Science*. 2008;319(5865):916–919.
18. Sondo E, Pesce E, Tomati V, Marini M, Pedemonte N. RNF5, DAB2 and friends: novel drug targets for cystic fibrosis. *Curr Pharm Des*. 2017;23(1):176–186.
19. Okiyoneda T, et al. Mechanism-based corrector combination restores ΔF508-CFTR folding and function. *Nat Chem Biol*. 2013;9(7):444–454.
20. Farinha CM, et al. Revertants, low temperature, and correctors reveal the mechanism of F508del-CFTR rescue by VX-809 and suggest multiple agents for full correction. *Chem Biol*. 2013;20(7):943–955.
21. Pedemonte N, et al. Small-molecule correctors of defective DeltaF508-CFTR cellular processing identified by high-throughput screening. *J Clin Invest*. 2005;115(9):2564–2571.
22. Van Goor F, et al. Rescue of DeltaF508-CFTR trafficking and gating in human cystic fibrosis airway primary cultures by small molecules. *Am J Physiol Lung Cell Mol Physiol*. 2006;290(6):L1117–L1130.
23. Mendoza JL, et al. Requirements for efficient correction of ΔF508 CFTR revealed by analyses of evolved sequences. *Cell*. 2012;148(1–2):164–174.
24. Rabeh WM, et al. Correction of both NBD1 energetics and domain interface is required to restore ΔF508 CFTR folding and function. *Cell*. 2012;148(1–2):150–163.
25. Goldstein AL, Goldstein AL. From lab to bedside: emerging clinical applications of thymosin alpha 1. *Expert Opin Biol Ther*. 2009;9(5):593–608.
26. Romani L, et al. Thymosin α1 represents a potential potent single-molecule-based therapy for cystic fibrosis. *Nat Med*. 2017;23(5):590–600.
27. De Stefano D, et al. Restoration of CFTR function in patients with cystic fibrosis carrying the F508del-CFTR mutation. *Autophagy*. 2014;10(11):2053–2074.
28. Tosco A, et al. A novel treatment of cystic fibrosis acting on-target: cysteamine plus epigallocatechin gallate for the autophagy-dependent rescue of class II-mutated CFTR. *Cell Death Differ*. 2016;23(8):1380–1393.
29. Ma T, et al. Thiazolidinone CFTR inhibitor identified by high-throughput screening blocks cholera toxin-induced intestinal fluid secretion. *J Clin Invest*. 2002;110(11):1651–1658.
30. Scudieri P, et al. Association of TMEM16A chloride channel overexpression with airway goblet cell metaplasia. *J Physiol (Lond)*. 2012;590(23):6141–6155.
31. Carlin JM, Ozaki Y, Byrne GI, Brown RR, Borden EC. Interferons and indoleamine 2,3-dioxygenase: role in antimicrobial and antitumor effects. *Experientia*. 1989;45(6):535–541.
32. Zegarra-Moran O, Folli C, Manzari B, Ravazzolo R, Varesio L, Galietta LJ. Double mechanism for apical tryptophan depletion in polarized human bronchial epithelium. *J Immunol*. 2004;173(1):542–549.
33. Besançon F, Przewlocki G, Baró I, Hongre AS, Escande D, Edelman A. Interferon-gamma downregulates CFTR gene expression in epithelial cells. *Am J Physiol*. 1994;267(5 Pt 1):C1398–C1404.
34. Galietta LJ, et al. Modification of transepithelial ion transport in human cultured bronchial epithelial cells by interferon-gamma. *Am J Physiol Lung Cell Mol Physiol*. 2000;278(6):L1186–L1194.
35. Bebok Z, et al. Failure of cAMP agonists to activate rescued deltaF508 CFTR in CFBE41o- airway epithelial monolayers. *J Physiol (Lond)*. 2005;569(Pt 2):601–615.
36. Pedemonte N, et al. Dual activity of aminoarylthiazoles on the trafficking and gating defects of the cystic fibrosis transmem-

brane conductance regulator chloride channel caused by cystic fibrosis mutations. *J Biol Chem*. 2011;286(17):15215–15226.
37. Sondo E, et al. Rescue of the mutant CFTR chloride channel by pharmacological correctors and low temperature analyzed by gene expression profiling. *Am J Physiol, Cell Physiol*. 2011;301(4):C872–C885.
38. Pesce E, et al. Synthesis and structure-activity relationship of aminoarylthiazole derivatives as correctors of the chloride transport defect in cystic fibrosis. *Eur J Med Chem*. 2015;99:14–35.
39. Tomati V, et al. Genetic inhibition of the ubiquitin ligase Rnf5 attenuates phenotypes associated to F508del cystic fibrosis mutation. *Sci Rep*. 2015;5:12138.
40. Pesce E, et al. Evaluation of a systems biology approach to identify pharmacological correctors of the mutant CFTR chloride channel. *J Cyst Fibros*. 2016;15(4):425–435.
41. Gentzsch M, Cui L, Mengos A, Chang XB, Chen JH, Riordan JR. The PDZ-binding chloride channel ClC-3B localizes to the Golgi and associates with cystic fibrosis transmembrane conductance regulator-interacting PDZ proteins. *J Biol Chem*. 2003;278(8):6440–6449.
42. Mall M, et al. The DeltaF508 mutation results in loss of CFTR function and mature protein in native human colon. *Gastroenterology*. 2004;126(1):32–41.
43. Kreda SM, et al. Characterization of wild-type and deltaF508 cystic fibrosis transmembrane regulator in human respiratory epithelia. *Mol Biol Cell*. 2005;16(5):2154–2167.
44. Cui L, et al. Domain interdependence in the biosynthetic assembly of CFTR. *J Mol Biol*. 2007;365(4):981–994.
45. Kreda SM, Gentzsch M. Imaging CFTR protein localization in cultured cells and tissues. *Methods Mol Biol*. 2011;742:15–33.
46. Guo Y, et al. Thymosin alpha 1 suppresses proliferation and induces apoptosis in breast cancer cells through PTEN-mediated inhibition of PI3K/Akt/mTOR signaling pathway. *Apoptosis*. 2015;20(8):1109–1121.
47. Lao X, et al. A modified thymosin alpha 1 inhibits the growth of breast cancer both in vitro and in vivo: suppressment of cell proliferation, inducible cell apoptosis and enhancement of targeted anticancer effects. *Apoptosis*. 2015;20(10):1307–1320.
48. Pier GB, Grout M, Zaidi TS. Cystic fibrosis transmembrane conductance regulator is an epithelial cell receptor for clearance of Pseudomonas aeruginosa from the lung. *Proc Natl Acad Sci USA*. 1997;94(22):12088–12093.
49. Gee HY, Noh SH, Tang BL, Kim KH, Lee MG. Rescue of ΔF508-CFTR trafficking via a GRASP-dependent unconventional secretion pathway. *Cell*. 2011;146(5):746–760.
50. Fulcher ML, Randell SH. Human nasal and tracheo-bronchial respiratory epithelial cell culture. *Methods Mol Biol*. 2013;945:109–121.
51. Hild M, Jaffe AB. Production of 3-D airway organoids from primary human airway basal cells and their use in high-throughput screening. *Curr Protoc Stem Cell Biol*. 2016;37:IE.9.1–IE.9.15.